Available online at www.sciencedirect.com
ScienceDirect
Journal of Magnetic Resonance 188 (2007) 10–23
JMR Journal of Magnetic Resonance
www.elsevier.com/locate/jmr

A novel improved method for analysis of 2D diffusion–relaxation data—2D PARAFAC-Laplace decomposition

Erik Tønning [a,*], Daniel Polders [b], Paul T. Callaghan [c], Søren B. Engelsen [a]

[a] *Quality & Technology, Department of Food Science, Faculty of Life Sciences, University of Copenhagen, Rolighedsvej 30, DK-1958 Frederiksberg C, Denmark*[1]

[b] *Laboratory for Biophysics, Wageningen University and Research Centre, Dreijenlaan 1, 6703 HA Wageningen, The Netherlands*[2]

[c] *MacDiarmid Institute for Advanced Materials and Nanotechnology, Victoria University of Wellington, New Zealand*[3]

Received 26 March 2007
Available online 8 June 2007

Abstract

This paper demonstrates how the multi-linear PARAFAC model can with advantage be used to decompose 2D diffusion–relaxation correlation NMR spectra prior to 2D-Laplace inversion to the T_2–D domain. The decomposition is advantageous for better *interpretation* of the complex correlation maps as well as for the *quantification* of extracted T_2–D components. To demonstrate the new method seventeen mixtures of wheat flour, starch, gluten, oil and water were prepared and measured with a 300 MHz nuclear magnetic resonance (NMR) spectrometer using a pulsed gradient stimulated echo (PGSTE) pulse sequence followed by a Carr–Purcell–Meiboom–Gill (CPMG) pulse echo train. By varying the gradient strength, 2D diffusion–relaxation data were recorded for each sample. From these double exponentially decaying relaxation data the PARAFAC algorithm extracted two unique diffusion–relaxation components, explaining 99.8% of the variation in the data set. These two components were subsequently transformed to the T_2–D domain using 2D-inverse Laplace transformation and quantitatively assigned to the oil and water components of the samples. The oil component was one distinct distribution with peak intensity at $D = 3 \times 10^{-12}\ \mathrm{m^2\ s^{-1}}$ and $T_2 = 180$ ms. The water component consisted of two broad populations of water molecules with diffusion coefficients and relaxation times centered around correlation pairs: $D = 10^{-9}\ \mathrm{m^2\ s^{-1}}$, $T_2 = 10$ ms and $D = 3 \times 10^{-13}\ \mathrm{m^2\ s^{-1}}$, $T_2 = 13$ ms. Small spurious peaks observed in the inverse Laplace transformation of original complex data were effectively filtered by the PARAFAC decomposition and thus considered artefacts from the complex Laplace transformation. The oil-to-water ratio determined by PARAFAC followed by 2D-Laplace inversion was perfectly correlated with known oil-to-water ratio of the samples. The new method of using PARAFAC prior to the 2D-Laplace inversion proved to have superior potential in analysis of diffusion–relaxation spectra, as it improves not only the interpretation, but also the quantification.

Keywords: DRCOSY; PARAFAC; Laplace inversion; Diffusion; Relaxation; Correlation spectroscopy; NMR; PGSTE; Dough; Water; Oil

1. Introduction

Characterisation of water and fat components in food is of prime importance due to its modulation of important properties such as taste, texture, oxidation and shelf life. Diffusion correlated NMR relaxometry is a unique technique for characterisation of dynamics, compartmentalisation and phases of fat and water in food, as it is able to measure complex solid or semi-solid food matrices such as meat, cheese, dough and bread. This correlation technique, in which 2D-Laplace inversion NMR is used to provide a map in T_2–D space, is used to analyse the complex multi-exponential behaviour of the relaxation and diffusion rates in heterogeneous systems. It enables us to obtain a plot that is easy to interpret and separates components of a system via their dynamics, revealing additional informa-

* Corresponding author. Fax: +45 35283245.
E-mail address: ert@life.ku.dk (E. Tønning).
[1] http://www.models.life.ku.dk.
[2] http://www.bip.wur.nl/UK.
[3] http://www.macdiarmid.ac.nz/nmr.

1090-7807/$ - see front matter © 2007 Elsevier Inc. All rights reserved.
doi:10.1016/j.jmr.2007.05.018

tion by correlating these molecular motions when compared with a 1D technique [1–3].

2D diffusion–relaxation data are double-exponentially decaying landscapes and thus second order data structures. Data from series of complex samples can with advantage be analysed using multi-way chemometric methods, as these will provide for unique resolution of pure component landscapes. Multi-way analysis has successfully been applied in several chemical fields including fluorescence emission–excitation spectroscopy [4] and 2D NMR spectroscopy [5,6]. The key issue in multi-way analysis is to have access to boxes of data rather than tables of data. Usually, a single spectrum is recorded for each sample. Data for several samples are then gathered in a matrix/table. If, instead, the data are recorded as a function of two variables (e.g. residual magnetisation as a function of time, yielding relaxation, and as a function of magnetic field gradient, yielding diffusion), then the data from one sample are contained in a matrix. For several samples a box of data is obtained. Such multi-way data can be modelled with specialized tools that take particular advantage of the data structure. Most notably, the so-called PARAFAC model [7] is an interesting alternative to traditional data analysis tools, because it allows resolving complex mixture measurements into the pure single-component spectra. The advantage of PARAFAC in this context is its ability to provide unique solutions to data that are approximately multi-linear. T_2–D weighted relaxation data is one example of trilinear data. These can be decomposed by PARAFAC into a few pure and unique physico-chemical components with exactly the same data structure as the original data. A subsequent T_2–D Laplace inversion of the resolved components will then provide the T_2–D distribution profile of the pure components. The PARAFAC algorithm thus works as a filter, extracting only the systematic variation from a coherent set of DRCOSY recordings, while leaving out the non-systematic variation in the residuals. The combined method constitutes a significant improvement to the complex T_2–D Laplace inversion of individual samples in which the researcher has no objective means of assessing if individual peaks represent physico-chemical components or artefacts that appear due to the ill-conditioned problem and unfortunate choice of regularisation. A conceptual sketch of the new composite method demonstrated in this paper is shown in Fig. 1.

2. Theory

The correlated measurement of diffusion and spin relations by NMR requires the use of an r.f. and magnetic field gradient pulse train which "encodes" for both parameters on the same nuclear spin magnetisation. The separate encoding methods for diffusion and relaxation are described in detail elsewhere [8]. The combined DRCOSY method uses a pulsed gradient stimulated echo (PGSTE) [9,10] followed by a Carr–Purcell–Meiboom–Gill (CPMG) pulse echo train [11,12]. During that CPMG train the spin magnetisation signal, M, relative to the initial echo amplitude, M_0, is sampled, both as a function of time, t, during the train, and gradient strength, q^2 applied in the PGSTE sequence before the train. This the signal is acquired in a 2D (t, q^2) space as:

$$\frac{M(t,q^2)}{M_0} = \sum p(D,T_2)\mathrm{e}^{-q^2D(\Delta-\frac{\delta}{3})}\mathrm{e}^{\frac{-t}{T_2}} + \mathrm{e}(t,q^2) \quad \text{and} \quad q = G\gamma\delta, \tag{1}$$

where Δ is the diffusion observation time, γ is the gyromagnetic ratio, δ is the gradient duration and G is the gradient strength. Eq. (1) thus assumes a distribution of diffusion coefficients, D, and relaxation times, T_2, with joint probability, p [13].

In order to obtain the distribution p, the experimental data must be inverted using 2D-Laplace inversion. This is done according to Song et al. (2002) [14] by considering a the discrete matrix form of Eq. (1):

$$\mathbf{M} = \mathbf{K_1}\mathbf{X}\mathbf{K_2'} + \mathbf{E} \tag{2}$$

where $\mathbf{K}_1$ and $\mathbf{K}_2$ are the known matrices of the exponentials in Eq. (1) for the observation time and gradient strengths used while *choosing* a discrete number of relaxation times and diffusion coefficients in a specified range. Thus, the window of observation and resolution is chosen by the investigator and the applicability (robustness) limits of the algorithm. $\mathbf{X}$ is the unknown T_2–D distribution matrix extracted by minimising:

$$\chi^2 = \|\mathbf{M} - \mathbf{K_1}\mathbf{X}\mathbf{K_2'}\|^2 + \alpha\|\mathbf{X}\|^2 \tag{3}$$

where α is a regularisation factor set by the user depending on the desired smoothness of the result and $\|\cdot\|$ is the Frobenius norm. Choosing an appropriate α is not straightforward; however, when following the usual guidelines [14], in which α is adjusted to just minimize χ^2, the results are often readily interpretable. In contrast to the PARAFAC model, the Laplace inversion problem is ill-conditioned and depends on the algorithm used for regularisation and the set of parameters used. Thus, caution must be taken when interpreting and quantifying peaks in the T_2–D spectra.

In this work we aim to investigate if the inherent labile nature of the Laplace inversion procedure can be improved by resolving (filtering) the unique components using the PARAFAC algorithm [7] prior to the 2D-Laplace transformation of the data. Using parallel factor analysis (PARAFAC) we stack the 2D landscapes of the different samples in a 3D array, $\underline{\mathbf{M}}$, of the size: $I \times J \times K$. I is the number of samples, J is the number of gradient steps and K is the number of time points. If the data is tri-linear, each observation point, m_{ijk} in $\underline{\mathbf{M}}$, can be described uniquely as:

$$m_{ijk} = \sum_{f=1}^{F} a_{if}b_{jf}c_{kf} + e_{ijk}, \quad i = 1,\ldots,I; \quad j = 1,\ldots,J; \quad k = 1,\ldots,K \tag{4}$$

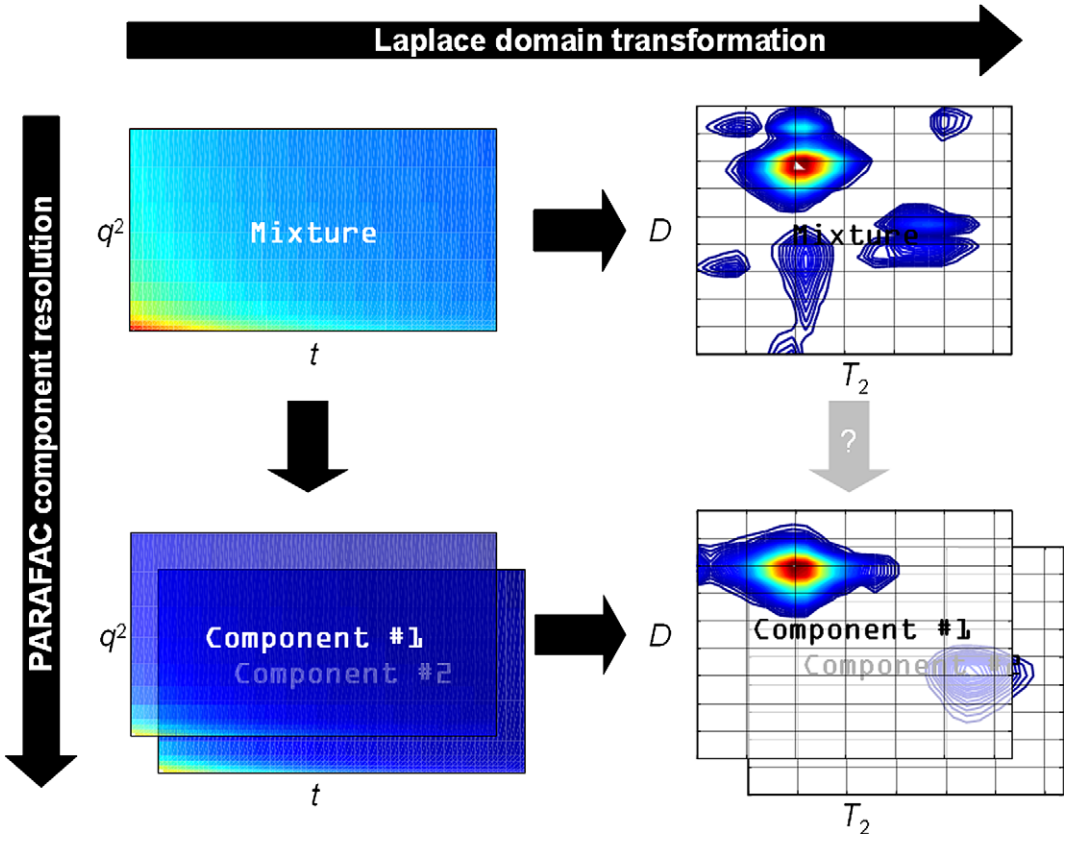

Fig. 1. Concept scheme of the method demonstrated. Raw 2D diffusion–relaxation NMR data (upper left) can be directly transformed into the T_2–D domain (upper right) by Laplace inversion or as suggested here via spectral decomposition by PARAFAC (lower left) to unique T_2–D PARAFAC-Laplace components (lower right).

where F is the number of PARAFAC components, $\mathbf{a}_f$, $\mathbf{b}_f$ and $\mathbf{c}_f$ are the PARAFAC scores of lengths I, J and K, respectively, and a_{if} is the ith element of $\mathbf{a}_f$, b_{jf} is the jth element of $\mathbf{b}_f$ and c_{kf} is the kth element of $\mathbf{c}_f$. A graphical representation of the PARAFAC model with two components is found in Fig. 2, where $\underline{\mathbf{M}}$ is the original box of data. Mode 1 is samples, mode 2 is relaxation time, t, and mode 3 is the gradient strength, q^2. PARAFAC decomposes the data into two unique components consisting of three loading vectors, one for each mode, and a residual matrix, $\underline{\mathbf{E}}$. By taking the outer product of loading 2, $\mathbf{b}_f$, and loading 3, $\mathbf{c}_f$, of each component the components are now represented by a 2D-loading spectrum with an associated sample loading, $\mathbf{a}_f$, holding the concentrations of the components of in each sample. The sample loading vectors are also termed score vectors. Thus each sample is now decomposed into a weighted sum of unique 2D diffusion–relaxation spectra and a residual matrix. The weights are the sample scores in mode 1.

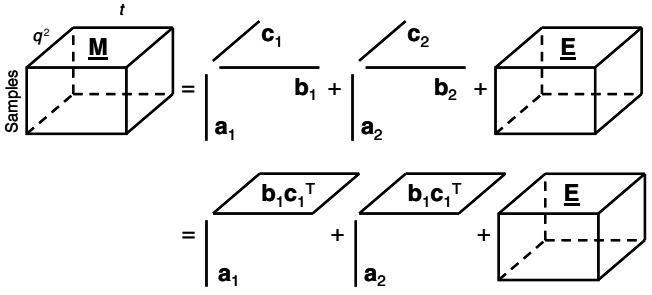

Fig. 2. Graphical representation of a 3-way array, $\underline{\mathbf{M}}$, decomposed by PARAFAC into two unique components and a residual, $\underline{\mathbf{E}}$. See text for thorough explanation.

Eq. (4) is completely unaffected by the underlying distributions in Eq. (1) of the pure physico-chemical components, as the PARAFAC algorithm is not restricted by the mathematical relationship within the components. PARAFAC simply extracts independently varying additive components. The prerequisite for this extraction is, that a number of samples is recorded in a manner by which the components of interest are purposely varied either by design or by natural variation.

The aim of this investigation is to demonstrate that PARAFAC in practice is able to resolve pure 2D diffusion–relaxation components on a set of samples containing the same components, but in different proportions. When this is achieved and the quantification is thus in place, interpretation is straightforward by subsequent application of the 2D Laplace inversion to the pure 2D diffusion–relaxation components. The hypothesis is that application of PARAFAC will facilitate a more direct interpretation and robust application of the 2D Laplace inversion. The

particular experimental system used comprises wheat doughs. This system was chosen, because it provides sufficient complexity in the T_2–D spectrum and because of the inherent interest in developing robust 2D-inverse Laplace methods for the food industry.

3. Experimental

3.1. Materials

Five wheat flour samples from a Danish/German field experiment were used. They were chosen for their diverse quality with respect to baking quality and functionality. An even greater diversification of samples in this investigation was obtained by mixing the following ingredients: wheat starch (Unmodified, Sigma CAS 9005-25-8), wheat gluten (Sigma, CAS 8002-80-0), commercially available soy oil and commercially available high-grade wheat flour available in New Zealand (trademark: Champion).

3.2. Characterisations

An extensive characterisation of the Danish/German wheat flours was performed for other purposes and will be elaborated elsewhere. The mixing property with regards to water uptake was investigated using a Farinograph according to ICC standard No. 115/1. The commercially available flour was characterised using a Foss NIRS (near-infrared reflectance spectroscopy) Bench Analyser with an in-house calibration at Weston Milling, Lower Hutt, Wellington for estimation of several parameters including moisture and Farinograph water absorption. The water content of the flours as well as the starch and the gluten were determined by gravitational method prior to mixing the doughs. Two gram of the materials were dried at 130 °C for 1.5 h and scaled before and after according to ICC standard No. 110/1 (Table 1).

3.3. Dough preparations

Twelve samples were prepared by mixing wheat starch, wheat gluten and soy oil following a full factorial design with three centre points (Fig. 3) and with the commercially available wheat flour as filler to a 43 g dm sample, i.e. equal to 50 g sample at 14% moisture. The factorial ingredients were used in three levels each: starch: 0, 10.0 and 20.0 g dm; gluten: 0, 3.5 and 7.0 g dm; oil: 0, 1.0 and 2.0 g (Fig. 3). The dry matter mass of commercial flour was thus dependent on the levels of pure ingredients and varied between 14.0 and 43.0 g dm. To all mixtures 30 g of water was added, thus assuming an average of 60% water uptake based on 14% moisture in all the mixtures. The sum of the moisture contents of the ingredients and the added water in the samples added up to 37 g in all mixtures equal to 46% of the total mass (Table 1). The mixed samples were prepared and recorded in random order. The Danish/German wheat flour samples were included for natural variation in the experimental setup (Fig. 3). They were only mixed with water according to their water absorption and actual moisture content (Table 1).

A 50MDD Laboratory Mixer, Lincoln, New Zealand was used for preparing the doughs. In the running mixer the flour samples and, respectively, the mixture samples were added to the mixing chamber. The ingredients of the mixture samples were added consecutively in the following order: flour, starch, gluten and soy oil. After tempering at 34 °C for 2 min the dough preparation was initiated by adding water (34 °C) in amounts corresponding to the water absorption capacity and the energy counter was simultaneously reset. The doughs were mixed for 49–259 s depending on the dough consistency development until the energy input reached 10.0 Wh/kg dough. The aim of the procedure was to add an equal amount of work into each sample and thus to produce samples in a uniform and reproducible way.

3.4. NMR recordings

Immediately after preparation a small amount of dough was inserted bit by bit into a 5 mm wide NMR tube using a piston rod to pack the material while avoiding air bubbles to form. The tube was filled up to 3 cm in order to fully cover the sampling area of the tube. The tube was inserted into a Bruker Avance 300 System fitted with a Bruker 36 T m^{-1} gradient coil, capable of applying a strong specific perturbation of the magnetic field along the z direction. The machine was operated from a UNIX PC running xwinnmr version 3.6.

A DRCOSY pulse program was written consisting of a pulsed gradient stimulated echo (PGSTE) followed by a Carr–Purcell–Meiboom–Gill (CPMG) echo train (Fig. 4). The $\pi/2$ and π hard pulses were applied for 5.2 and 10.4 μs, respectively. The PGSTE was initiated by a $\pi/2$ hard pulse, initiating a free induction decay (FID) followed by a magnetic field gradient pulse, two consecutive $\pi/2$ hard pulses and a magnetic field gradient pulse of exactly the same size as the first after which a stimulated echo occurs depending on the size of the gradient. The peak intensities of echoes were then recorded during a CPMG sequence.

In 25 consecutive PGSTE+CPMG runs the gradient strength was varied from 0 to 12.96 T m^{-1} in 25 approximately exponentially spaced steps with constant diffusion observation time, $\Delta = 20.00$ ms and gradient duration, $\delta = 2.00$ ms with ramp times of 500 μs in 10 steps, i.e. ramp up time of 500 μs, stable time of 1500 μs and ramp down time of 500 μs. The q-encoding gradient pulses were flanked by delays of 500 μs immediately before and after the gradient. The latter was applied specifically to allow for the ring down of induced eddy currents in the surrounding metals before applying the 2nd $\pi/2$ hard pulse, the spin-conserving pulse. During the z-storage time of 16,489.6 μs before the 3rd $\pi/2$ hard pulse a crusher gradient (homospoil) was ramped in 4 steps of 50 μs to 5% of

Table 1
Twelve mixtures named by their contents of starch (S), gluten (G), fat (F) denoted by 0, 1 and 2 for levels zero, medium and high, respectively

Sample #	ID	Quantities of ingredients (% moisture)							Mixing time	Totals		
		Starch (11.2%) (g)	Gluten (7.9%) (g)	Fat (—) (g)	Flour (12.9%) (g)	Moist. in mixture (%)	Water upt. (14% moist.) (%)	Water added (g)		Sample mass (g)	Water (%)	Added fat (%)
S01	S0G0F0	0.0	0.00	0.0	49.4	12.9	60.0	30.6	01:05	80.0	46.3	0.00
S02	S0G2F0	0.0	7.60	0.0	41.3	12.1	60.0	31.1	00:49	80.0	46.3	0.00
S03	S2G0F0	22.5	0.00	0.0	26.4	12.1	60.0	31.1	01:55	80.0	46.3	0.00
S04	S2G2F0	22.5	7.60	0.0	18.4	11.3	60.0	31.5	01:12	80.0	46.3	0.00
S05	S0G0F2	0.0	0.00	2.0	47.1	12.3	60.0	30.9	01:57	80.0	46.3	2.50
S06	S0G2F2	0.0	7.60	2.0	39.0	11.6	60.0	31.4	01:14	80.0	46.3	2.50
S07	S2G0F2	22.5	0.00	2.0	24.1	11.6	60.0	31.4	04:19	80.0	46.3	2.50
S08	S2G2F2	22.5	7.60	2.0	16.1	10.8	60.0	31.8	01:42	80.0	46.3	2.50
S09	S2G2F2	22.5	7.60	2.0	16.1	10.8	60.0	31.8	02:19	80.0	46.3	2.50
S10	S1G1F1	11.3	3.80	1.0	32.7	11.8	60.0	31.2	01:27	80.0	46.3	1.25
S11	S1G1F1	11.3	3.80	1.0	32.7	11.8	60.0	31.2	01:27	80.0	46.3	1.25
S12	S1G1F1	11.3	3.80	1.0	32.7	11.8	60.0	31.2	01:34	80.0	46.3	1.25
S13	03KCF3	—	—	—	50.1	14.1	58.9	29.4	01:24	79.5	45.9	0.00
S14	03AVF3	—	—	—	50.3	14.5	53.5	26.5	00:55	76.8	44.0	0.00
S15	04KCF1	—	—	—	49.8	13.6	58.6	29.5	01:21	79.3	45.8	0.00
S16	04AVF1	—	—	—	49.8	13.7	52.5	26.4	01:17	76.3	43.6	0.00
S17	04APRf	—	—	—	49.8	13.6	61.2	30.8	01:21	80.6	46.7	0.00

Flour is added to obtain a 43 g dm sample and water is added assuming a 60% water uptake (based on 14% water) for all mixtures. Five additional samples flour of different origin, water content and water uptake is also included. Names refer to year (03/04), place (K, Kiel; A, Aarslev), cultivar (C, Carbo; V, Vinjet; P, Pentium) and treatment (F1, fraction 1; F3, fraction 3; Rf, Reference).

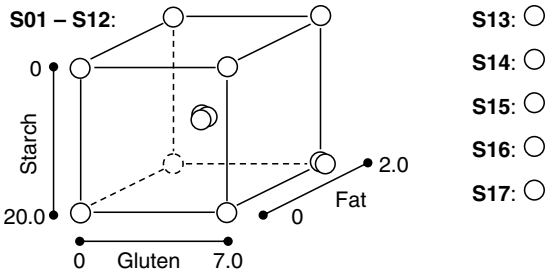

Fig. 3. The experimental design. Twelve mixture samples (S01–S12) in a full factorial design of experiment with three factors; Starch at 0, 10.0 and 20.0 g; gluten at 0, 3.5 and 7.0 g; soy oil at 0, 1.0 and 2.0 g. There are three centre points (S1G1F1) and the sample with high levels in all factors (S2G2F2) is represented twice. Five additional samples (S13–S17) are indicated. See Table 1 for details.

maximum gradient strength (i.e. 1.8 T m^{-1}) and kept for 1.0 ms before being ramped down again. By destroying unwanted transverse magnetisation the crusher effectively removed potential interference from the spin echo of the initial r.f. pulse-FID generated by the second hard pulse and thus also the FID from the second r.f. pulse that would otherwise become an echo after the third r.f. pulse. In order for the gradient to stabilise, i.e. reach steady state, ten dummy gradient pulses as described above, but without the hard pulses, were applied before the initial π/2 hard pulse.

The spin echo signal from the PGSTE pulse sequence was recorded during the subsequent CPMG pulse sequence with a time delay of 100 μs between the π hard pulses (10.4 μs) and the echo centres, thus the echo time, $\tau = 105.2$ μs. Three points in every second echo centre were recorded and subsequently averaged. Fourthousand and ninety-six even echoes were acquired during the 1.724 s CPMG pulse sequence. Four scans were made for every gradient step with a repetition delay of 1.977 s. The entire DRCOSY pulse sequence would thus run for 398.9 s.

3.5. Data processing

Data processing was performed using commercially available software packages, Prospa V2.0.12, Magritek, Wellington, New Zealand and Matlab Version 6.5 release 13, The MathWorks, Inc. Conversion and pre-processing of the data was made in Prospa as were the 2D-inverse Laplace transformations, while PARAFAC was run in Matlab using the *N*-way toolbox [15] from www.models.life.ku.dk. For every sample the resulting matrix of $25 \times (3 \times 4096)$ real and imaginary recordings was imported into Prospa. The three points in every echo were averaged and the real and imaginary recordings were summed. Since the DRCOSY pulse sequence does not produce meaningful data at zero gradient strength, the first data row was removed. The first column representing the initial echo recording was also removed due to deviating non-exponential values in the first of the three points recorded. Following this procedure the total data set was reduced to the dimensions: 17 samples × 24 gradient steps × 4095 acquisition times. As there was no internal standard and no control of the actual sample mass in the measured volume of the NMR tube, all samples were normalised with maximum intensity, i.e. the intensity of the first acquisition point assuming similar amounts of fast relaxation components in the samples.

For every gradient strength, G_i, the gradient axis values were calculated by:

$$\text{gradaxis}_i = q^2\left(\Delta - \frac{\delta}{3}\right) = (G_i\gamma\delta)^2\left(\Delta - \frac{\delta}{3}\right) \tag{5}$$

with the gyromagnetic ratio $\gamma = 2.675 \times 10^9$ s^{-1} T^{-1} and $G_{\min} = 0.216$ T m^{-1} and $G_{\max} = 12.96$ T m^{-1} the gradient axis thus spans from 0.258×10^9 to 929.447×10^9 s m^{-2}. The time axis associated with T_2 relaxation consisted of equidistant time point for every 420.8 μs corresponding to every 2nd echo beginning at time point 7.8416 ms corresponding to the actual duration of the two gradient pulses and the disregarded first echo. These axes were required when performing the 2D-inverse Laplace transformations in Prospa of the raw sample recordings as well as the PARAFAC components and residuals (see below).

A two-component PARAFAC model was calculated using non-negativity constraints in all three modes. For *each component* in *each sample* the three modes, intensity, a_{if}, time, $\mathbf{b}_f$, and gradient, $\mathbf{c}_f$, were subsequently multiplied: $a_{if}\mathbf{b}_f\mathbf{c}_f^T$, as illustrated in Fig. 2. Thus, for each of the

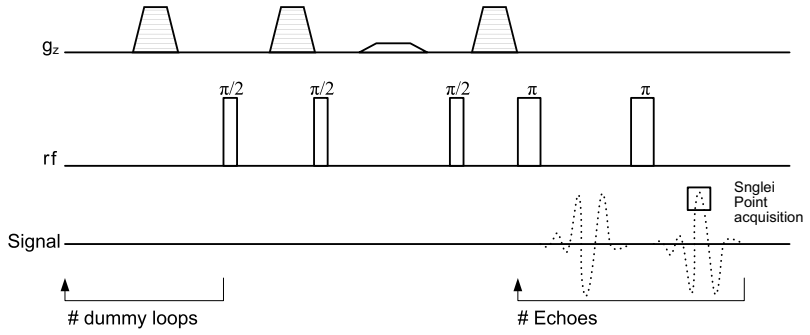

Fig. 4. The pulse program as used to collect the 2D diffusion–relaxation data. Effectively a PGSTE followed by a CPMG echo train, where acquisition is made at peak intensity for every 2nd echo.

seventeen samples, four 2D-matrices (raw, components 1 and 2 and the PARAFAC-residual) were produced and subsequently imported into Prospa. 2D-Laplace inversions were performed using the optimal regularisation factors, α, as determined by testing a range of reasonable values for each sample, component and residual (Fig. 8). T_2 and D axes, i.e. the observation window, were chosen as follows: $T_{2,\min} = 1 \times 10^{-3}$ s, $T_{2,\max} = 1.5$ s, $D_{\min} = 1 \times 10^{-16}$ m^2 s^{-1} and $D_{\max} = 1 \times 10^{-7}$ m^2 s^{-1} in 24 logarithmically spaced steps in both directions. The T_2 and D boundaries were chosen purposely too wide to include T_2–D space where no intensities should be observed. This helps in determining the quality of fit, keeping the elasticity of the regularisation factor in mind.

T_2–D correlation pairs were identified from the resulting spectra of raw data, components 1 and 2 and the PARAFAC residuals from each sample and quantified by their sum relative to total spectral intensity of each raw sample spectrum, respectively. The qualitative as well as the quantitative aspects were compared for two selected samples and the intensity ratios of components 1 to component 2 were compared to the known ratios of oil and water in the samples.

4. Results and discussion

The major variation introduced in this investigation was imposed by the factorial design varying the major components, starch, gluten and fat of wheat dough, while keeping the water concentration constant. This was, however, not the case of the additional flour samples that included only natural variation and water concentration corresponding to the optimal water absorption (Table 1). Despite the relatively complex composition of dough with protons associated with carbohydrates, protein, fat and water, it was expected that only protons associated with molecules with high rotational and translational (diffusion) freedom could be observed in this experiment. Thus, only water and oil components were expected, possibly influenced by the proportions of other components, i.e. starch and gluten, of the mixture. Wheat flour contains 1.5–2.5% lipids of which roughly one third is mono-, di- and tri-glyceride lipids, one third is starch lipids and one third is bound lipids (glycolipids and phospholipids). In dough, glycolipids and gluten-bound phospholipids are thought to form a laminar phase, stabilising a micro-emulsion of free phospholipids and acyl lipids in water all encapsulated by the gluten network [16].

Table 1 lists the mixture proportions of the samples. The assumed water absorption of 60% in the commercial flour was not correct, as the true value was determined to 64.1%. However, this is of no importance in the current study, since the optimal water absorption of the mixtures was unknown and the water absorption level was set merely to be able to form a visco-elastic dough, regardless of the proportions of starch, gluten, fat and flour. The varying mixing time thus reflects the variation in rheological properties of the various mixtures. As expected, high levels of starch and/or fat prolong the mixing time, while high levels of gluten hardens the dough, resulting in shorter mixing times. The diverse proportions of major ingredients were thus expected to create variation in the micro-environments for water and fat in the mixtures to be explored by the NMR recordings.

The PARAFAC model of the seventeen recorded double exponentially decays was derived from running the model with 1–4 components. The validity of the models was initially explored by simultaneous inspection of the loadings, the explained variance, core consistency and number of iterations [7,17]. From this exercise it was easily concluded that only a model with either two or three components could be valid. The two-component model had a core consistency of 100%, while that of the three-component model was close to 60%. By subsequent inspection of the loadings the third component displayed deviant behaviour from the exponential decay in the gradient mode and thus the two-component model was chosen. The chosen two-component model presented in Fig. 5 explains 99.8% of the variation in the entire data material.

In Fig. 5 the PARAFAC results were normalised to maximum intensity in the exponential decay modes (i.e. modes 2 and 3), thus leaving the relative variation in the sample mode for direct quantification of components (Fig. 5a). Due to the second order advantage of the PARAFAC algorithm the scores in mode 1 need only to be scaled to one reference value in order to give the pure component concentrations. In the two component PARAFAC model, component 1 scores were positively correlated with the added fat content, while component 2 scores were inversely correlated. Since the NMR recordings are only expected to return signals from oil and water, components 1 and 2 were quantitatively assigned to oil and water, respectively, on the basis of the scores (Fig. 5a). In mode 2, the relaxation time mode in Fig. 5b, two distinct exponentially decaying components are resolved; component 1 with a significantly slower decay than component 2, both decaying to approximately zero intensity. In mode 3, the gradient intensity mode in Fig. 5c, two distinct, apparently exponentially decaying components are observed; component 1 has a significantly slower diffusion than component 2. Component 2, however, clearly appears to be multi-exponential with a very slow diffusing covarying feature that does not reach zero intensity within the chosen limits of gradient strength.

A powerful visualisation taking the outer product as illustrated in Fig. 2 of the individual component vectors from mode 2 and mode 3 of the two PARAFAC components is presented in Fig. 5d and e. The combined correlated decays are readily visualised for further interpretation by transformation to the T_2–D domain. It is thus possible by PARAFAC to decompose raw 2D-decays from each sample into their pure components and a sample specific residual matrix. This is done in the left columns of Figs. 6 and 7 for two markedly different samples, S01: S0G0F0 and S08: S2G2F2, presented with equal

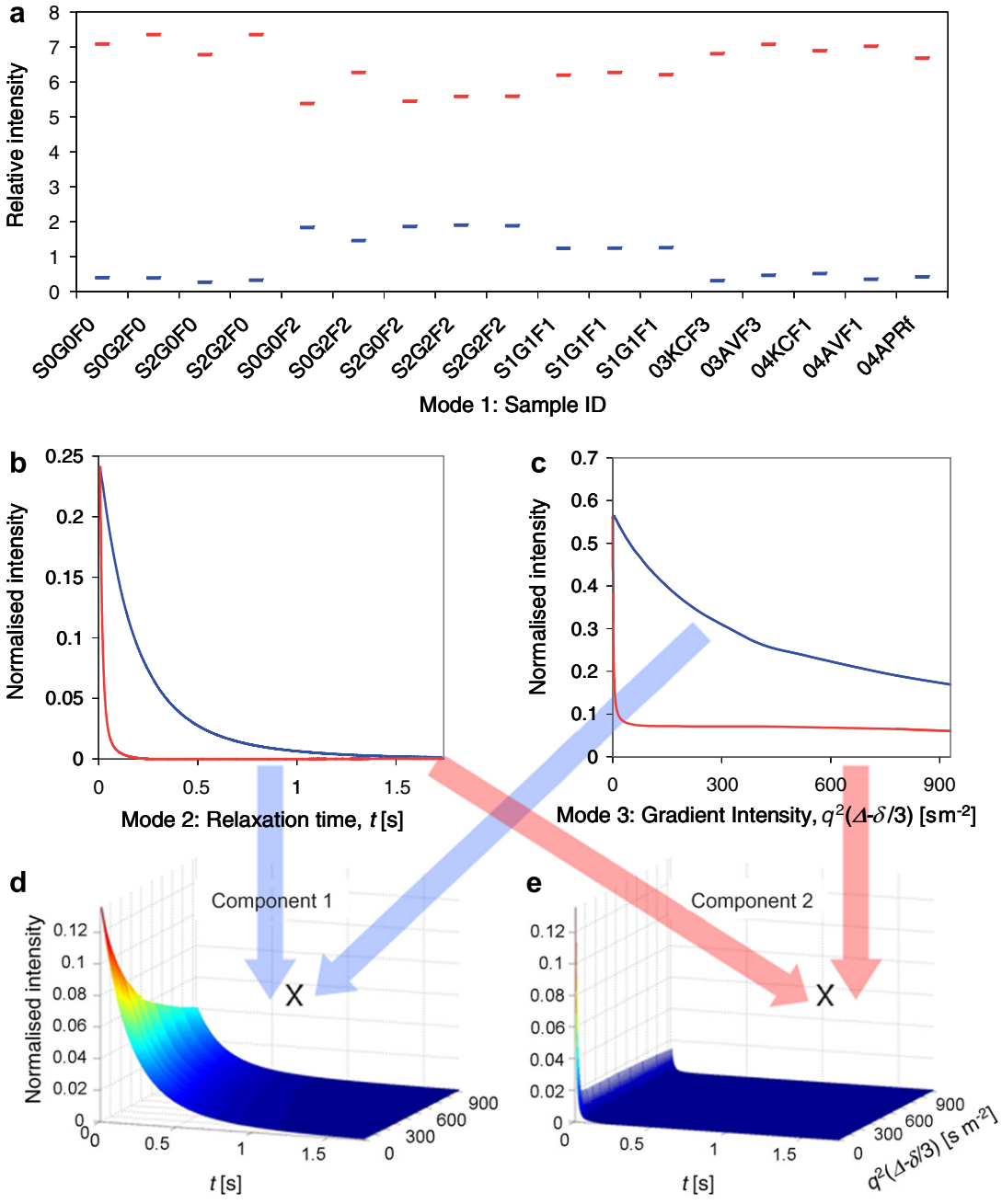

Fig. 5. Two component PARAFAC model of DRCOSY data. — (blue) Component 1, — (red) Component 2. (a) Mode 1: Relative intensities (scores) of components 1 and 2 for each individual sample/mixture. (b) Mode 2: Normalised intensities of components 1 and 2 in the relaxation time direction. (c) Mode 3: Normalised intensities of components 1 and 2 in the gradient direction. (d) and (e) The two DRCOSY components are visualised by taking the outer products of respective components in modes 2 and 3. This figure is equivalent to Fig. 2 explaining the PARAFAC decomposition. (For interpretation of the references to color in this figure legend, the reader is referred to the web version of this paper.)

scaling for proportional interpretation. For interpretation and further quantification the raw data, the two components and the residual 2D-data are transformed into the T_2–D domain by 2D-Laplace inversion in the right column. Figs. 6 and 7 are thus the actual decomposition conceptually presented in Fig. 1.

In Fig. 6 sample S01: S0G0F0 is presented both in the time-gradient domain and in the T_2–D domain. From the raw data (Fig. 6a) it is quite clear that the data is composed of both fast and slow diffusing features as well as fast and slow relaxation features. By the 2D-Laplace inversion (Fig. 6b) this is nicely visualised as nine peaks as T_2–D pairs along with their approximate relative intensities listed in Table 2. Peaks with less than 1% of maximum intensity are not represented in the figure nor in the table, for which reason the sum of listed peaks only sums to 99.1%. In comparison, sample S08: S2G2F2 displays eight peaks in Fig. 7b. Peaks P1–P7 are common for both S01 and S08,

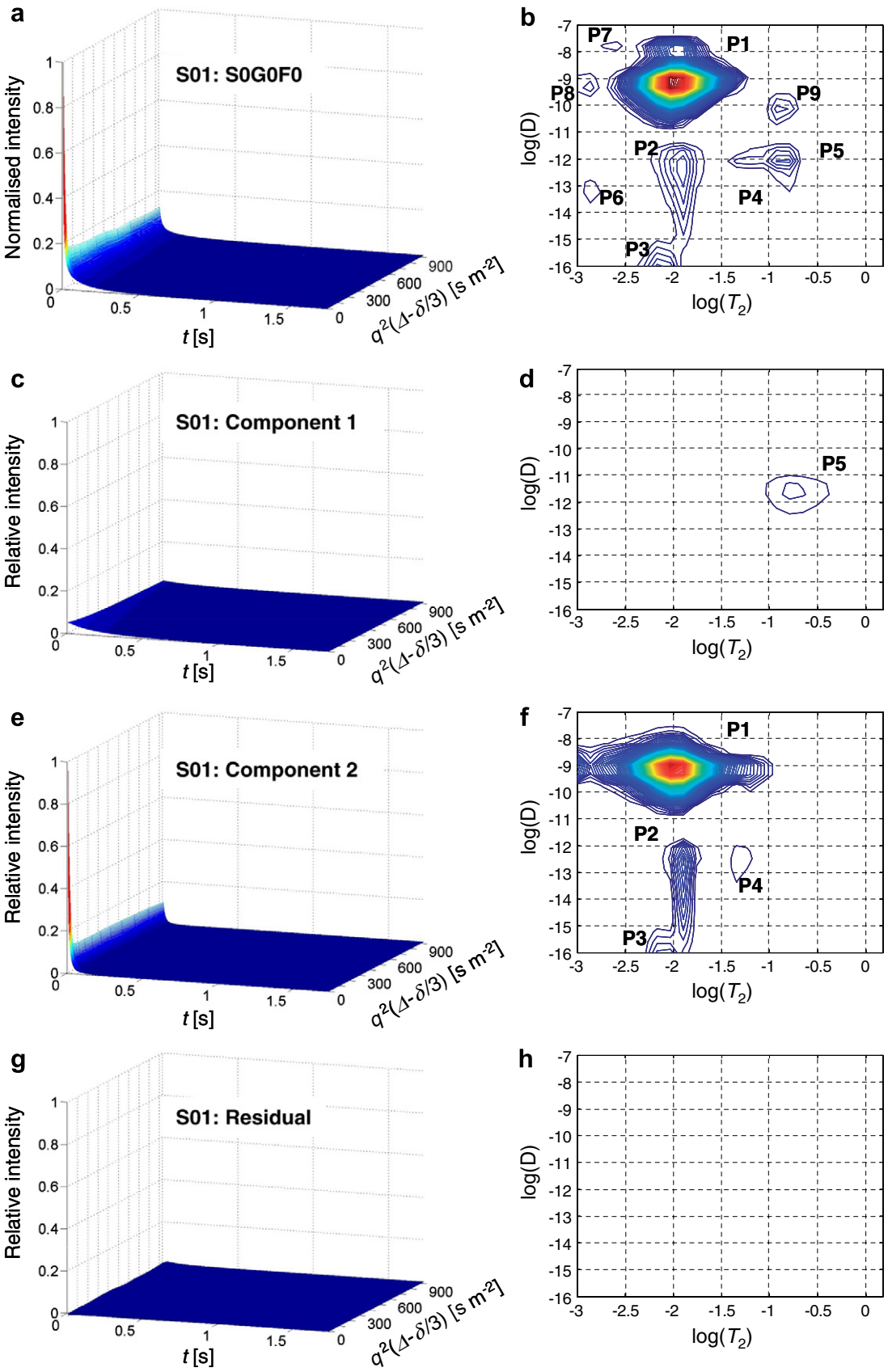

Fig. 6. Sample S01: S0G0F0 split quantitatively into its PARAFAC components 1 + 2 and residual (left column) presented with their corresponding T_2–D correlation maps obtained by 2D-Laplace inversion (right column). Every contour line in the right panels represents additional 1% of maximum intensity.

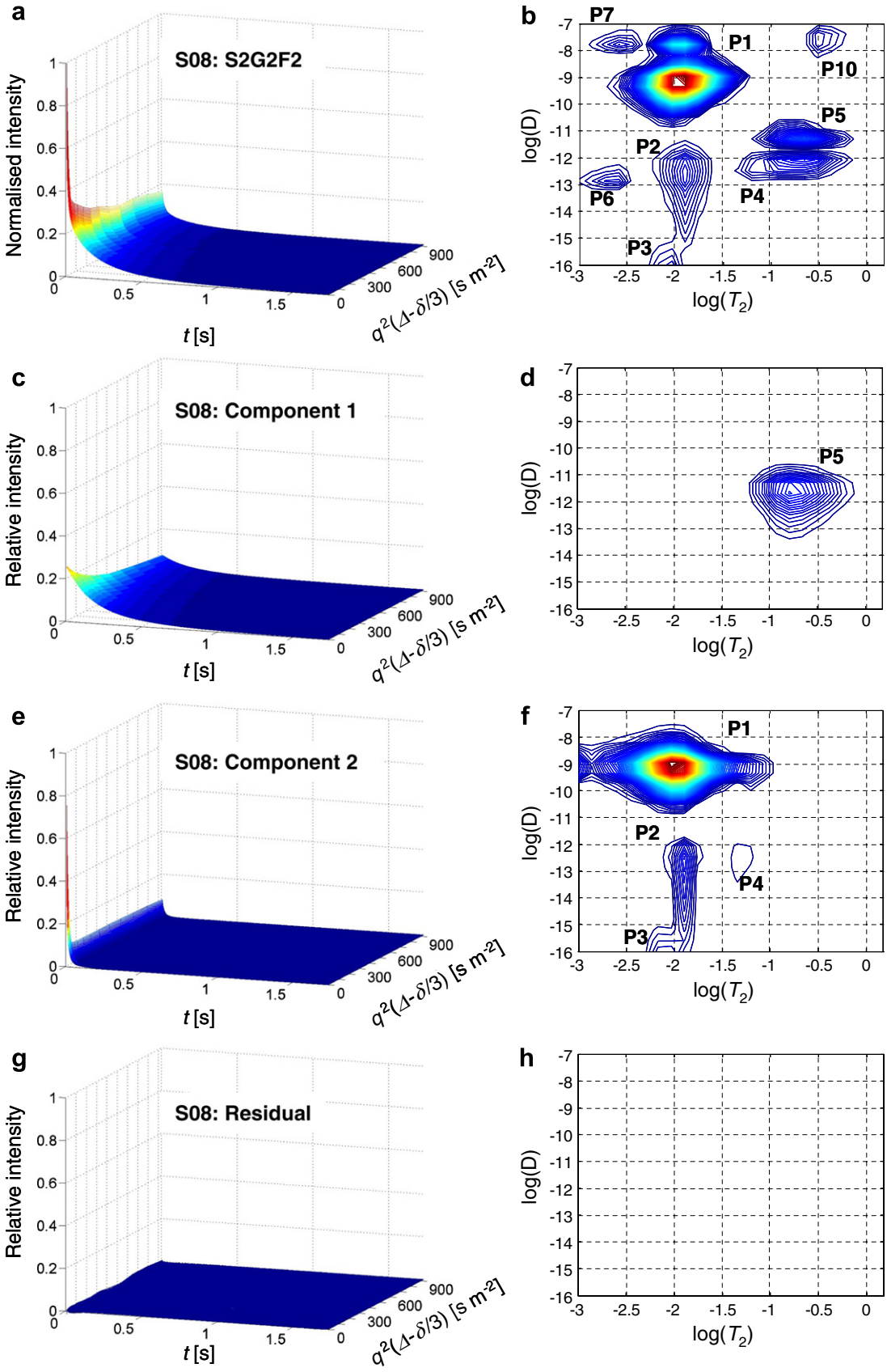

Fig. 7. Sample S08: S2G2F2 split quantitatively into its PARAFAC components 1 + 2 and residual (left column) presented with their corresponding T_2–D correlation maps obtained by 2D-Laplace inversion (right column). Every contour line in the right panels represents additional 1% of maximum intensity.

Table 2
Intensities of peaks P1–P10 as identified in Figs. 6 and 7 in the T_2–D domain for sample S01 and S08

Peak	T_2 [ms]	D[m^2 s^{-1}]	S01: S0G0FO					S08: S2G2F2				
			Raw	PARAFAC				Raw	PARAFAC			
				Comp 1 (%)	Comp 2 (%)	Residual (%)	Sum (%)		Comp 1 (%)	Comp 2 (%)	Residual (%)	Sum (%)
Total int	All	All	100.0	2.2	102.5	0.1	104.8	100.0	12.0	92.8	1.4	106.2
P1	10	1×10^{-9}	88.6		95.9		95.9	78.1		86.8		86.8
P2	13	3×10^{-13}	4.5		4.3		4.3	6.4		3.9		3.9
P3	6	1×10^{-16}	1.5		1.6		1.6	0.9		1.5		1.5
P4	50	1×10^{-12}	0.6		0.6		0.6	0.6		0.6		0.6
P5	180	1×10^{-12}	1.8	2.2			2.2	10.2	12.0			12.0
P6	1.6	5×10^{-14}	0.6				0.0	1.4				0.0
P7	2.5	1.5×10^{-8}	0.2				0.0	1.1				0.0
P8	1.3	5×10^{-10}	0.5				0.0	0.0				0.0
P9	130	8×10^{-11}	0.8				0.0	0.1				0.0
P10	300	3×10^{-8}	0.0				0.0	1.1				0.0
Sum			99.1	2.2	102.5	0.0	104.6	99.6	12.0	92.7	0.0	104.8
Residual			0.9	0.0	0.0	0.1	0.1	0.4	0.0	0.0	1.4	1.4

Intensities are presented as relative to total intensity of the respective raw spectrum. Peaks are summed leaving an unrealised residual for each spectrum, i.e. Raw, Comp 1, Comp 2 and PARAFAC-Residual. The PARAFAC-Laplace peaks are summed horizontally.

while P8 and P9 are only present in S01 and P10 is present only in S08.

The challenges in the interpretation of the similarities and deviations of these and the remaining samples are overwhelming, although some delimitation can be put forward by manual inspections. Peaks with diffusion coefficient higher than say 10^{-8} m^2 s^{-1} must be considered noise, since the limit of diffusion in this system must be considered to be the diffusion of free water, i.e. 2×10^{-9} m^2 s^{-1}. Likewise, peaks below $T_2 = 10$ ms are unlikely, since the duration of the pulsed gradient time (7 ms) and the storage time (16.5 ms) would probably render such signals extinct prior to the first recordings by the CPMG train. Thus, P6, P7, P8 and P10 in Figs. 6b and 7b are artefacts due to noise and the ill-conditioned Laplace inversion. P3 is a typical border phenomenon due to a small offset in the raw data along the gradient direction. Thus, by reasoning it is possible to reduce the problem to five peaks of interest. Apart from peak P9 present only in S01, all relevant peaks are present in both samples. P1 is by far the most intense with 88.6% for S01 and 78.1% for S08 (Table 2) and considering the high diffusion coefficient it must be water being able to move freely in the matrix, although restricted in rotational freedom ($T_2 = 10$ ms), thus probably associated with the surfaces of the matrix, i.e. the gluten network. P2 at 4.5% and 6.4%, respectively, equally restricted in rotational freedom is much more restricted in diffusion with a broad distribution of diffusion coefficients that indicate tightly bound water, probably associated with water absorption by swelling starch granules. P4 is very small, 0.6% for both, and only identified as a peak due to the new method (see Section 4 below). P5 varies markedly between the two samples, 1.8% in S01 and 10.2% in S08, proportional with the difference in oil content for the two samples. In Fig. 7b, S08 peak P5 forms a double peak which will be discussed below. With $D = 10^{-12}$ and $T_2 = 180$ ms P5 is most probably fat restricted in diffusion by the size of the vesicles in the water matrix and at the same time with more slow relaxation than the "free" water molecules.

4.1. Qualitative analysis

We will now demonstrate the experiment interpretation from the point of view of the new method. The samples S01 and S08 were decomposed into the two PARAFAC components (Figs. 6c, e and 7c, e) corresponding to their relative amounts in the raw data and the sample-specific non-systematic residual (Figs. 6g and 7g). The residual is the difference between original sample recording and the PARAFAC components. While transforming the PARAFAC components 1 and 2 and the residual rather than the raw data by 2D-Laplace inversion only common structures to the entire set of samples are investigated (Figs. 6d, f, h and 7d, f, h). Keeping in mind that 99.8% of all the variation in the set of 2D-multi-exponential data is explained by just two PARAFAC components justifies this approach when investigating these data.

First we observe that only peaks P1–P5 are represented in the PARAFAC-Laplace components 1 (Fig. 6d, f) and 2 (Fig. 7d, f). The residuals did not contain any significant exponential behaviour, which was also the case for all other samples and accordingly the T_2–D plots are empty (Figs. 6h and 7h). Component 1 contains one peak only (Figs. 6d and 7d)—the P5 fat component described above. Being a PARAFAC component shows that this component varies between samples independently from the other components. This is in fine accordance with the fact that oil content was varied purposely in the design of the experiment. PARAFAC-Laplace component 2 in Figs. 6f and 7f contains P1–P4, in which P4 was only recognised in its own right by this method. In the T_2–D spectra of the raw data this was not readily observed, as this peak was both small and overlapping with P5. The PARAFAC-Laplace decom-

position thus shows that the water found in three different compartments in the matrix is highly covarying, which in turn indicates that the water compartmentalisation in this study of dough at 34 °C is highly unaffected by the proportions of starch, gluten and oil. In Table 2 the proportionate intensities of the peaks in the PARAFAC-Laplace components are presented relative to total intensity of the summed peaks of the *raw* Laplace data. Due to the non-uniqueness and labile character of the Laplace algorithm these intensities do not add up to 100%—but relatively close. The relative proportions of the components (Component 1/Component 2) in S01, 2.2%/102.5% directly correspond to the summed proportions, 1.8%/95.2% in the spectrum of the raw data as in the S08 case where the 12.0%/92.7% component ratio corresponds to the 10.2%/86.0% ratio of the summed raw data. This quantitatively confirms that the PARAFAC-Laplace decomposition is equivalent to ordinary direct 2D-Laplace inversion. The relative quantitative information is conserved.

The fact that the two components when transformed into the T_2–D domain have only a few distinct features suggests that other features found (i.e. P6–P10) in the individual raw spectra are only artefacts inflated by the ill-conditioned properties of the Laplace inversion. The Laplace inversion estimates many parameters based on one sample only which gives a poor independent variable to parameter ratio. Although every 2D-landscape is generated from multiple scans of thousands of data points, they are strongly covarying, thus giving a single error the possibility to be inflated by the data analysis. Artefacts from unfortunate sample presentation in the spectrometer, such as different packing of the material, air bubbles or bad mixing of the sample may turn up in the spectra and mistakenly be interpreted as components. PARAFAC resolvation prior to 2D-Laplace inversion significantly reduces these artefacts by the inherent second order advantage of reducing noise and uniquely extracting pure covarying components.

The optimal regularisation factor in the 2D-Laplace inversion was calculated independently for raw sample spectra, PARAFAC components 1 and 2 and PARAFAC residuals individually. A high factor produces results with many sharp features, while a low factor produces a smooth result. The optimum is somewhere in between, where the residual variance expressed by χ^2 is close to the mathematical optimum, i.e. lowest obtainable value that at the same time produces relatively smooth and interpretable plots. The actual regularisation chosen is somewhat subjective and based on experience. From Fig. 8 the regularisation factors were chosen to the nearest order of magnitude. Note that χ^2 for the PARAFAC residuals did not vary significantly in the α-plot, as it is noise being modelled by the 2D-Laplace inversion algorithm with no or insignificant exponential behaviour left. In practice, the regularisation factor is quite difficult to determine from sample to sample, but should ideally be the same for all samples in order to interpret and compare spectra, i.e. with the same smoothness independent of the variations in signal-to-noise ratio from sample to sample.

The signal/noise ratios for the PARAFAC components do not vary from sample to sample, as they are represented in all samples—just in different proportions. This leads to a key point that only these two—not seventeen α's need to be determined, i.e. $\alpha_{opt} = 10^8$ for component 1 and $\alpha_{opt} = 10^9$ for component 2 (Fig. 8). The fact that components 1 and 2 use different regularisation factors is due to their difference in intensity and thus different signal/noise ratio. In this example the most intense component dominates when determining the regularisation of the raw sample data. This is nicely illustrated by the samples presented in Figs. 6b and 7b in which peak, P5, appears as a single peak in T_2–D spectrum of S01, while it is a double peak in S08. The water peak, P1, is the dominant signal and will as an apparent optimum choose $\alpha_{raw} = 10^9$ (Fig. 8), even though this value is not optimal in relation to the weaker peak(s). Thus, non-significant features and noise in the data lead to confusing sharp peaks, double peaks (Fig. 7b) and non-physical peaks in spectra. On the other hand, focusing on the weaker peaks in the raw data by choosing a smaller α would eliminate non-physical peaks, but at the same time broaden the more intense peak(s) and even intercept smaller true peaks. PARAFAC analysis prior to the 2D-Laplace inversion elegantly solves this dilemma by separating the true physico-chemical components prior to the change of domain by Laplace inversion.

Because artefacts are introduced by the Laplace transformation as described above and because the choice of regularisation factor plays a significant role depending on the signal/noise ratios of the sample spectra the theoretically possible route of running PARAFAC in the T_2–D domain as indicated in Fig. 1 by arrow with a question mark was quickly abandoned.

4.2. Quantitative analysis

The ratio between oil and water can be studied quantitatively, and these data are presented in Fig. 9. A theoretical ratio is calculated from a commonly accepted level of acyl lipids in flour (0.7%) and the amount of fat which was added to the samples. In both water and oil the approximate number of H-atoms relative to molecular mass is 1/9, thus the relative abundance of fat–H to water–H can be calculated directly by their masses and by their presence in the DRCOSY data. Component 1 versus component 2 ratios are plotted for each sample directly from the PARAFAC scores in mode 1 (Fig. 5a) as well as from PARAFAC-Laplace spectra of the same components and summed to total intensity as done for S01 and S08 in Table 2.

Fig. 9 shows the quantitative ratio determined by the PARAFAC scores as well as PARAFAC-Laplace volumes of the components 1 and 2. They are both perfectly correlated ($r = 0.971$) with calculated oil/water ratios in the samples. In the calculation of the natural oil content the

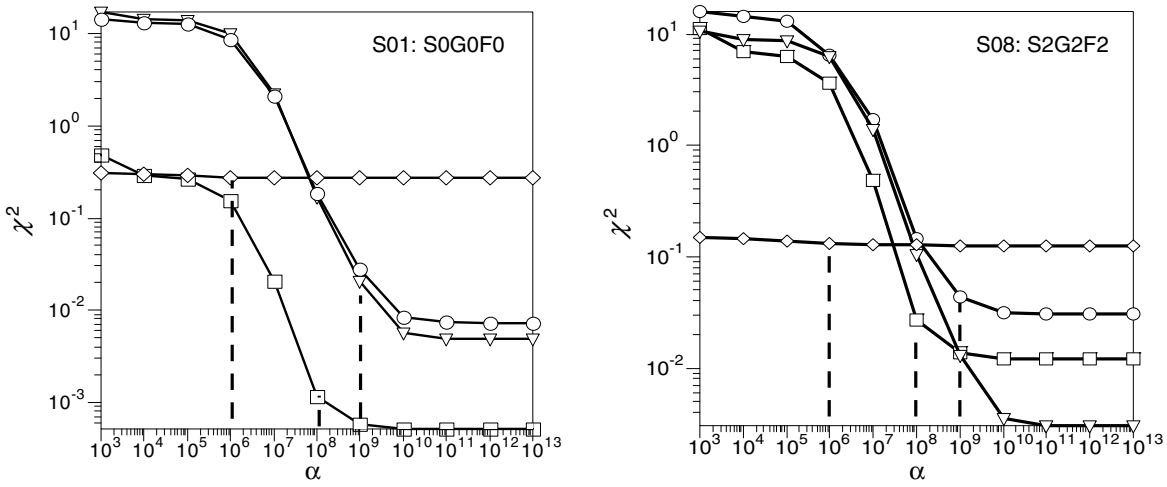

Fig. 8. Residual variance, χ^2 as a function of regularisation factor, α for sample S01: S0G0F0 and S08: S2G2F2: Raw data (○) $\alpha_{opt} = 10^9$, PARAFAC-component 1 (□) $\alpha_{opt} = 10^8$, PARAFAC-component 2 (∇) $\alpha_{opt} = 10^9$ and the PARAFAC-residual (◇) $\alpha_{opt} = 10^6$.

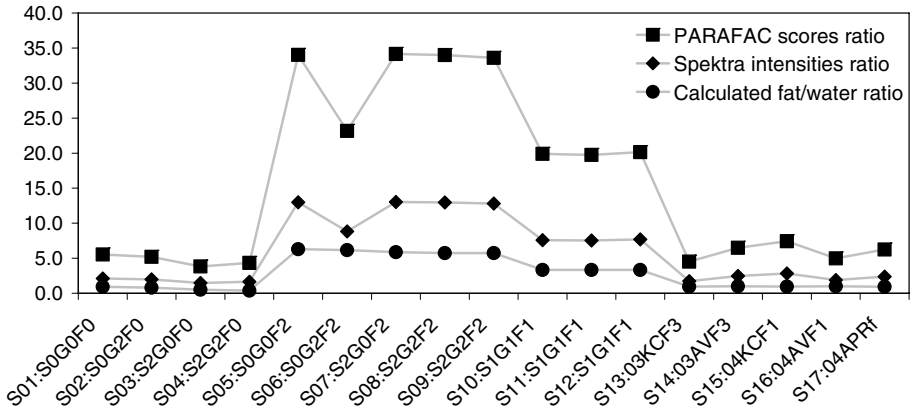

Fig. 9. Calculated water/oil ratios plotted with PARAFAC scores ratios and PARAFAC-Laplace volume ratios of component 1/component 2.

average oil contribution from flour (0.7%) was included as an offset. However, the gluten added in the mixtures may also contain significant amounts of lipids, as these are usually not easily extracted from gluten without destroying the gluten [16]. However, as no quantitative information was available, the eventual gluten bound fat was neglected in the calculations. The PARAFAC scores ratio and the summed PARAFAC-Laplace volume ratios of the two components are perfectly correlated, i.e. $r = 1.000$, because the 2D-Laplace inversion is performed on the exact same two components for each sample. Thus, for pure quantification purposes the Laplace domain transformation may actually be superfluous.

The PARAFAC scores ratios in Fig. 9 do not overlap the calculated fat/water ratios, because the PARAFAC analysis cannot take the relaxation during gradient encoding in the first 7.8416 ms into account. Fast relaxing compounds (say, $T_2 < 20$ ms) are thus significantly underestimated. The ratios of the summed T_2–D spectra of the two components should ideally be exactly overlapping the calculated ratios. However, some of the water signal was probably lost during acquisition due to T_2 and T_1 relaxation during gradient and storage time.

In Fig. 9 sample S06: S0G2F2 indeed looks like an outlier (knowing the fat content to be high). This is probably due to bad mixing or packing of the material in the tube prior to the recording. However, this outlying sample does not destroy the PARAFAC-Laplace model—it is only the proportions of water and oil that seem unlikely, taking prior knowledge into account. When leaving this sample out of the model, the correlation coefficient between the calculated and the PARAFAC estimated fat/water ratios was: $r = 0.997$.

Although both the PARAFAC ratios and the spectra ratios of the components are far from the known fat/water content, the near 100% correlation with known fat/water ratio is useful. Knowing the actual fat/water ratio of just one sample, the remaining samples can be calculated from the PARAFAC scores ratios, even if the fast relaxing water relaxation signal was not recorded quantitatively. That is the 2nd order advantage which is of great value in cases where the method of recording the signal, i.e. the

DRCOSY, cannot be set optimally for quantitative recording of the signals from fast relaxing components. As long as all 2D diffusion–relaxation spectra are recorded identically, relative comparisons are always possible based on the PARAFAC scores only. The unique PARAFAC resolvation of all varying components is based on having 2D-matrices of data for each sample, rather than just 1D-vectors.

5. Conclusions

The method combining the unsupervised PARAFAC model with 2D Laplace inversion has shown to be a significant improvement in the analysis of two-dimensional multi-exponential data recorded by DRCOSY. It allows identification and quantification of pure components and it reduces artefacts and stabilises the subsequent 2D Laplace inversion. This approach supports research by identifying real systematically varying components while filtering artefacts associated with unfavourable conditioning of the Laplace inversion.

The new procedure can be regarded as a step towards automatic analysis of DRCOSY and similar data as an alternative to biased human interpretation. The analysis requires a homologous set of samples in which specific factors of interest have been varied either by experimental design or by natural diversity of the materials investigated. In a future publication we will demonstrate that double SLICING [18–20] can be used to extract discrete T_2–D components from a single COSY recording.

Acknowledgments

A number of institutions, private companies and individuals are greatly acknowledged: The MacDiarmid Institute at Victoria University Wellington, New Zealand for providing time, space and knowledge; Allan K. Hardacre, Crop & Food Research, Palmerston North, New Zealand for good discussions and providing equipment. Bala Diagaradjan, Weston Milling, Lower Hutt, Wellington, New Zealand for reference analysis on short notice; Cerealia Mills, Vejle, Denmark for facilitating laboratory space and equipment in the milling process. For financial support we are greatly thankful to DFFE with the project title ''Un-entangling complex food systems by NMR/US spectroscopy and mathematical modelling'' sponsored by the Ministry of Food, Agriculture and Fisheries, to the Interreg IIIA programme between Fyns Amt, Odense, Denmark and Technologie-Region K.E.R.N, Rendsburg, Germany and to University of Copenhagen, Faculty of Life Sciences, Frederiksberg, Denmark for financing first author's Ph.D scholarship. Special thanks to Q-Interline Spectroscopic Analytical Solutions, Roskilde, Denmark, Knud Højgaards Fond, Charlottenlund, Denmark and Danmarks Jordbrugsvidenskabelige Ph.D-forening, Copenhagen, Denmark for travel Grants making the visit to Wellington possible for the first author.

References

[1] P.T. Callaghan, S. Godefroy, B.N. Ryland, Use of the second dimension in PGSE NMR studies of porous media, Magn. Reson. Imaging 21 (2003) 243–248.
[2] P.L. Hubbard, P.J. Watkinson, L.K. Creamer, A. Gottwald, P.T. Callaghan, Two-dimensional Laplace inversion NMR technique applied to the molecular properties of water in dry-salted mozzarella-type cheeses with various salt concentrations, in: S.B. Engelsen, P.S. Belton, H.J. Jakobsen (Eds.), Magnetic resonance in food science. The multivariate challenge. The proceedings of the 7th international conference on applications of magnetic resonance in food science held in Copenhagen on the 13–15th September 2004, The Royal Society of Chemistry, Cambridge, UK, 2005, pp. 225–232.
[3] Y. Qiao, P. Galvosas, P.T. Callaghan, Diffusion correlation NMR spectroscopy study of anisotropic diffusion of water in plant tissues, Biophys. J. 89 (4) (2005) 2899–2905.
[4] J. Christensen, L. Nørgaard, R. Bro, S.B. Engelsen, Multivariate autofluorescence of intact food systems, Chem. Rev. 106 (6) (2006) 1979–1994.
[5] R. Bro, P.I. Hansen, N. Viereck, M. Dyrby, H.T. Pedersen, S.B. Engelsen, A new principle for unique spectral decomposition of 2D NMR data, in: S.B. Engelsen, P.S. Belton, H.J. Jakobsen (Eds.), Magnetic resonance in food science. The multivariate challenge. The proceedings of the 7th international conference on applications of magnetic resonance in food science held in Copenhagen on the 13–15th September 2004, The Royal Society of Chemistry, Cambridge, UK, 2005, pp. 195–203.
[6] H.T. Pedersen, M. Dyrby, S.B. Engelsen, R. Bro, Application of multi-way analysis to 2D NMR data, Annu. Rep. NMR Spectrosc. 59 (2006) 207–233.
[7] R. Bro, PARAFAC. Tutorial and applications, Chemom. Intell. Lab. Syst. 38 (2) (1997) 149–171.
[8] P.T. Callaghan, Principles of Nuclear Magnetic Resonance Microscopy, Clarendon Press, Oxford, 1991.
[9] E.L. Hahn, Spin echoes, Phys. Rev. 80 (4) (1950) 580–594.
[10] J.E. Tanner, Use of the stimulated echo in NMR diffusion studies, J. Chem. Phys. 52 (1970) 2523–2526.
[11] H.Y. Carr, E.M. Purcell, Effects of diffusion on free precession in nuclear magnetic resonance experiments, Phys. Rev. 94 (1954) 630–638.
[12] S. Meiboom, D. Gill, Modified spin-echo method for measuring nuclear relaxation times, Rev. Sci. Instrum. 29 (1959) 688–691.
[13] M.D. Hurlimann, L. Venkataramanan, C. Flaum, The diffusion-spin relaxation time distribution function as an experimental probe to characterize fluid mixtures in porous media, J. Chem. Phys. 117 (2002) 10223–10232.
[14] Y.-Q. Song, L. Venkataramanan, M.D. Hürlimann, M. Flaum, P. Frulla, C. Straley, T_1–T_2 correlation spectra obtained using fast two-dimensional laplace inversion, J. Magn. Res. 154 (2002) 261–268.
[15] C.A. Andersson, R. Bro, The *N*-way Toolbox for MATLAB. Chemom. Intell. Lab. Syst. 52(1) (2000) 1–4, <http://www.models.life.ku.dk/source/nwaytoolbox/>.
[16] H.-D. Belitz, W. Grosch, Food Chemistry, second ed., Springer, Verlag, Berlin, 1999.
[17] C.A. Andersen, R. Bro, Practical aspects of PARAFAC modelling of fluorescence excitation-emission data, J. Chemom. 17 (4) (2003) 200–215.
[18] H.T. Pedersen, R. Bro, S.B. Engelsen, Towards rapid and unique curve resolution of low-field NMR relaxation data: trilinear SLICING versus two-dimensional curve fitting, J. Magn. Res. 157 (2002) 141–155.
[19] S.B. Engelsen, R. Bro, PowerSlicing, J. Magn. Res. 163 (2003) 192–197.
[20] C. Manetti, C. Castro, J.P. Zbilut, Application of trilinear SLICING to analyse a single relaxation curve, J. Magn. Res. 168 (2004) 273–277.